# Threshold Voltage Model for a Fully Depleted SOI-MOSFET with a Non-Uniform Profile

Zhang Guohe†, Shao Zhibiao, and Zhou Kai

(*Department of Electronic Science & Technology, Xi'an Jiaotong University, Xi'an 710049, China*)

**Abstract**: A novel approximation of the two-dimensional (2D) potential function perpendicular to the channel is proposed, and then an analytical threshold voltage model for a fully depleted SOI-MOSFET with a non-uniform Gaussian distribution doping profile is given based on this approximation. The model agrees well with numerical simulation by MEDICI. The result represents a new way and some reference points in analyzing and controlling the threshold voltage of non-uniform fully depleted (FD) SOI devices in practice.

**Key words**: fully depleted SOI-MOSFET; non-uniform; surface potential; threshold voltage
**EEACC**: 2520M; 2560B
**CLC number**: TN386 **Document code**: A **Article ID**: 0253-4177(2007)06-0842-06

## 1 Introduction

In recent years, fully depleted (FD) silicon-on-insulator (SOI) MOSFETs have attracted considerable attention because of their superior short-channel immunity[1] and ideal subthreshold characteristics[2]. There have been many reports on the modeling of the threshold voltage of these devices[3~8]. Young[3] assumed a second-order polynomial function for the potential perpendicular to the channel and derived a two-dimensional (2D) potential distribution in the SOI layer. Some other models that make this assumption have also been reported[4~8]. Yan *et al*.[4] developed Young's model and advanced a characteristic length associated with short-channel effects. However, this model does not depend on the buried-oxide thickness. Joachim *et al*.[5] pointed out that 2D effects in the buried-oxide layer could not be neglected for short-channel effects. Suzuki *et al*.[8] derived an analytical model for the threshold voltage for fully depleted single-gate SOI-MOSFETs, taking into consideration the 2D effects in both SOI and buried-oxide layers. This model matches the numerical data better than the previous ones.

The above models are all for uniformly concentrated doping in SOI films. Actually, the ion-implanted doping concentration of the film is considered to be non-uniform and is assumed to have a Gaussian distribution[9]. Ravariu *et al*.[10] advanced a one-dimensional (1D) model for the threshold of FD SOI-MOSFETs on films with a Gaussian profile. Pandey *et al*.[11] developed a new 2D threshold model for FD short-channel Si-SOI MESFETs with a non-uniform Gaussian profile.

In this paper, taking into consideration the 2D effects in both SOI and buried-oxide layers, an accurate 2D threshold voltage model for an FD SOI MOSFET with a non-uniform Gaussian doping concentration is derived by assuming a new potential function perpendicular to the channel.

## 2 Theoretical model

Figure 1 shows the vertical profile structure of an FD SOI MOSFET device, neglecting the source and drain regions. The notations are: $N_B(x)$ is the variable doping concentration in the p-type film; $N_{sub}$ is the uniform substrate doping concentration; $t_{oxf}$ is the front oxide thickness; $t_{si}$ is the SOI film thickness; $t_{oxb}$ is the buried-oxide thickness; $t_{sub}$ is the substrate thickness; $q$ is the electron charge; $\varepsilon_{si}$ is dielectric permittivity of silicon; and $\varepsilon_{ox}$ is the dielectric permittivity of the front oxide and buried-oxide. The depletion approximation for the SOI layer and substrate is

† Corresponding author. Email: ghzhang@stu.xjtu.edu.cn
Received 26 October 2006, revised manuscript received 29 January 2007

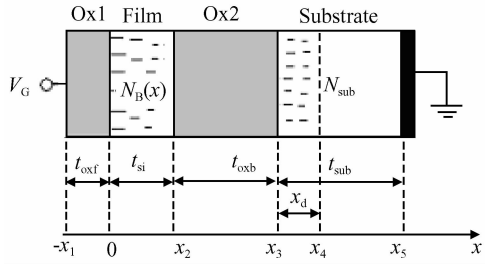


Fig.1　Vertical profile structure of FD SOI-MOSFET device

considered, and $x_d$ is the space charge region thickness in the substrate.

A Gaussian function is assumed for the variable doping concentration $N_B(x)$ in p-type film:

$$N_B(x) = N_p\exp\left[-\frac{1}{2}\times\left(\frac{x-R_p}{\sigma_p}\right)^2\right] \quad (1)$$

where $N_p$ is the peak concentration of the Gaussian doping profile, $R_p$ is the projected range, and $\sigma_p$ is the projected deviation.

The vertical potential distribution is derived by integrating the 1D Poisson's equation using boundary conditions that maintain the continuity of the electric flux and potential. The results are as follows:

For $x > x_4$, in the neutral region of the substrate,

$$\varphi(x) = 0 \quad (2)$$

For $x \in (x_3, x_4)$, in the depletion region of the substrate,

$$\varphi(x) = \frac{qN_{sub}}{2\varepsilon_{si}}(t_{si}+t_{oxb}+x_d-x)^2 \quad (3)$$

For $x \in (x_2, x_3)$, in the buried-oxide layer,

$$\varphi(x) = \frac{qN_{sub}}{\varepsilon_{si}}\times\frac{x_d^2}{2}+\frac{qN_{sub}}{\varepsilon_{ox}}(t_{si}+t_{oxb}-x)x_d \quad (4)$$

For $x \in (0, x_2)$, in the fully depleted SOI film,

$$\varphi(x) = \frac{qN_{sub}x_d^2}{2\varepsilon_{si}}+\frac{qN_{sub}x_d t_{oxb}}{\varepsilon_{ox}}+\frac{qN_{sub}(t_{si}-x)x_d}{\varepsilon_{si}}+\frac{\sqrt{\pi}qN_p\sigma_p^2\tau}{\varepsilon_{si}}[\mathrm{erf}(\tau)-\mathrm{erf}(A)]+\frac{qN_p}{\varepsilon_{si}}(e^{-\tau^2}-e^{-A^2}) \quad (5)$$

where $\tau=(x-R_p)\sqrt{2}\sigma_p$, $A=(t_{si}-R_p)/\sqrt{2}\sigma_p$.

For $x \in (-x_1, 0)$, in the forward oxide layer,

$$\varphi(x) = \left\{\frac{\sqrt{\pi}qN_p\sigma_p}{\sqrt{2}\varepsilon_{ox}}[\mathrm{erf}(B)-\mathrm{erf}(A)]-\frac{qN_{sub}x_d}{\varepsilon_{ox}}\right\}x+\frac{qN_{sub}}{2\varepsilon_{si}}x_d^2+\frac{qN_{sub}x_d}{\varepsilon_{ox}}(t_{oxb}+t_{si})-\frac{\sqrt{\pi}qN_p\sigma_p R_P}{\sqrt{2}\varepsilon_{si}}\times[\mathrm{erf}(B)-\mathrm{erf}(A)]+\frac{qN_p\sigma_p^2}{\varepsilon_{si}}(e^{-B^2}-e^{-A^2}) \quad (6)$$

where $B=-R_p/\sqrt{2}\sigma_p$, and the $x_d$ can be solved by applying a $V_G$ to the forward gate in Eq.(6).

The 2D Poisson equations for the potential in the channel region and buried-layer are

$$\frac{\partial^2\varphi_1(x,y)}{\partial x^2}+\frac{\partial^2\varphi_1(x,y)}{\partial y^2}=\frac{qN_B(x)}{\varepsilon_{si}},0<x<t_{si} \quad (7)$$

$$\frac{\partial^2\varphi_2(x,y)}{\partial x^2}+\frac{\partial^2\varphi_2(x,y)}{\partial y^2}=0,t_{si}<x<t_{si}+t_{oxb} \quad (8)$$

and Equation (7) can be changed to

$$\frac{1}{2\sigma_p^2}\times\frac{\partial^2\varphi_1}{\partial\tau^2}+\frac{\partial^2\varphi_1}{\partial y^2}=\frac{qN_p}{\varepsilon_{si}}e^{-\tau^2},\quad B<\tau<A \quad (9)$$

We have presented a new potential assumption for the non-uniform Gaussian doping profile. In the buried-oxide layer, we used a second-order polynomial potential.

$$\varphi_1(\tau,y) = C_{10}(y)+C_{11}(y)\tau+C_{12}(y)\left[\tau\mathrm{erf}(\tau)+\frac{e^{-\tau^2}}{\sqrt{\pi}}\right] \quad (10)$$

$$\varphi_2(x,y) = C_{20}(y)+C_{21}(y)x+C_{22}(y)x^2 \quad (11)$$

The constants $C_{10}$, $C_{11}$ and $C_{12}$ can then be determined by integrating Poisson's equation using the boundary conditions that maintain the continuity of the electric flux and potential. The potential at the surface of the SOI layer is $\phi_s$, and the electric field at the bottom of the SOI layer in the buried-oxide layer side is $E_b$, which depends on $y$. Then $C_{10}$, $C_{11}$ and $C_{12}$ are given by

$$C_{10}(y) = \phi_s - BC_{11}(y)-C_{12}(y)\left[B\mathrm{erf}(B)+\frac{1}{\sqrt{\pi}}e^{-B^2}\right] \quad (12)$$

$$C_{11}(y) = \frac{\sqrt{2}\sigma_p}{\mathrm{erf}(A)-\mathrm{erf}(B)}\times\left[-\frac{V_G'-\phi_s}{\gamma t_{oxf}}\mathrm{erf}(A)+\frac{E_b}{\gamma}\mathrm{erf}(B)\right] \quad (13)$$

$$C_{12}(y) = \frac{\sqrt{2}\sigma_p}{\mathrm{erf}(A)-\mathrm{erf}(B)}\left(\frac{V_G'-\phi_s}{\gamma t_{oxf}}-\frac{E_b}{\gamma}\right) \quad (14)$$

where $\gamma=\varepsilon_{si}/\varepsilon_{ox}$, $V_G'=V_G-V_{FB}$, $V_{FB}$ is the flat-band voltage.

Setting $\tau=A$ in Eq.(10), the potential at the bottom of the SOI layer $\phi_b$ can be obtained as

$$\phi_b = \phi_s-\frac{E_b}{\gamma}t_{si}+D\left[\frac{V_G'-\phi_s}{\gamma t_{oxf}}-\frac{E_b}{\gamma}\right] \quad (15)$$

where

$$D = \frac{\sqrt{2}\sigma_p[\exp(-A^2) - \exp(-B^2)]}{\sqrt{\pi}[\mathrm{erf}(A) - \mathrm{erf}(B)]} - R_p \tag{16}$$

Now we use boundary conditions in which the potentials and electric fluxes are continuous at the Si/buried-oxide interface, and the potential at the bottom of the buried-oxide layer is $\phi_{sb}$ which can be solved from Eq. (3). The constants $C_{20}$, $C_{21}$ and $C_{22}$ can then be determined, and Equation (11) reduces to

$$\varphi_2(x,y) = \frac{t_{oxb}^2 - t_{si}^2}{t_{oxb}^2}(\phi_b - \phi_{sb}) + \frac{t_{si}(t_{si} + t_{oxb})E_b}{t_{oxb}} + \phi_{sb} + \left[\frac{2t_{si}(\phi_b - \phi_{sb})}{t_{oxb}^2} - \frac{(2t_{si} + t_{oxb})E_b}{t_{oxb}}\right]x + \left(-\frac{\phi_b - \phi_{sb}}{t_{oxb}^2} + \frac{E_b}{t_{oxb}}\right)x^2 \tag{17}$$

According to Eqs. (10)～(17), the back potential $\phi_b$ can be determined by

$$\frac{\partial^2\phi_b}{\partial y^2} + \frac{V_G' - \phi_b}{\lambda_{gb}^2} = \frac{(\gamma t_{oxf} + t_{si})(V_G' - \phi_{sb})}{\lambda_{gb}^2(\gamma t_{oxf} + \gamma t_{oxb} + t_{si})} + \frac{r\sigma_p^2 t_{oxb}(\gamma t_{oxf} - D)(e^{-A^2} - e^{-B^2})}{\lambda_{gb}^2(D + R_p)(\gamma t_{oxf} + \gamma t_{oxb} + t_{si})} \times \frac{qN_p}{\varepsilon_{si}} \tag{18}$$

where $\lambda_{gb}$ is the characteristic length associated with $\phi_b$.

$$\lambda_{gb}^2 = \frac{\gamma t_{toxb}(\gamma t_{oxf} - D)}{2(D + R_p)(\gamma t_{oxf} + \gamma t_{oxb} + t_{si})} \times [2\sigma_p^2(1 - e^{A^2 - B^2}) + (D + R_p)t_{toxb}] \tag{19}$$

and the surface potential $\phi_s$ can be determined by

$$\frac{d^2\phi_s}{dy^2} + \frac{V_G' - \phi_s}{\lambda_{gf}^2} = \frac{\gamma t_{oxf}\sigma_p^2}{\lambda_{gf}^2(D + R_p)}(e^{-A^2} - e^{-B^2}) \times \frac{(\gamma t_{oxb} + t_{si} + D)}{(\gamma t_{oxf} + \gamma t_{oxb} + t_{si})} \times \frac{qN_p}{\varepsilon_{si}} + \frac{\gamma t_{oxf}(V_G' - \phi_{sb})}{\lambda_{gf}^2(\gamma t_{oxf} + \gamma t_{oxb} + t_{si})} \tag{20}$$

where $\lambda_{gf}$ is the characteristic length associated with the surface potential $\phi_s$ given by

$$\lambda_{gf}^2 = \frac{\gamma}{(D + R_p)(\gamma t_{oxf} + \gamma t_{oxb} + t_{si})[2\gamma\lambda_{gb}^2 t_{oxb} + (t_{si} + D)(2\lambda_{gb}^2 - t_{oxb}^2)]} \times \{t_{oxf}\sigma_p^2(\gamma t_{oxf} + \gamma t_{oxb} + t_{si})[2\gamma\lambda_{gb}^2 t_{oxb} + (t_{si} + D)(2\lambda_{gb}^2 - t_{oxb}^2)] \times (e^{B^2 - A^2} - 1) + \lambda_{gb}^2 t_{oxb}^3(\gamma t_{oxf} - D)(D + R_p)\} \tag{21}$$

By introducing the variable $\eta$ as

$$\eta = \phi_s - V_G + \left[\frac{\gamma t_{oxf}(V_G' - \phi_{sb})}{\gamma t_{oxf} + \gamma t_{oxb} + t_{si}} + \frac{qN_p}{\varepsilon_{si}} \times \frac{\gamma t_{oxf}\sigma_p^2(e^{-A^2} - e^{-B^2})(\gamma t_{oxb} + t_{si} + D)}{\lambda_{gf}^2(D + R_p)(\gamma t_{oxf} + \gamma t_{oxb} + t_{si})}\right] \tag{22}$$

Equation (20) can be reduced to

$$\frac{\partial^2\eta}{\partial y^2} - \frac{\eta}{\lambda_{gf}^2} = 0 \tag{23}$$

The boundary conditions for $\eta$ are

$$\eta(0) = V_{bi} - V_G' + \left[\frac{\gamma t_{oxf}(V_G' - \phi_{sb})}{\gamma t_{oxf} + \gamma t_{oxb} + t_{si}} + \frac{\gamma t_{oxf}\sigma_p^2(e^{-A^2} - e^{-B^2})(\gamma t_{oxb} + t_{si} + D)}{\lambda_{gf}^2(D + R_p)(\gamma t_{oxf} + \gamma t_{oxb} + t_{si})} \times \frac{qN_p}{\varepsilon_{si}}\right] \equiv \eta_S \tag{24}$$

$$\eta(L_G) = \eta_S + V_D \equiv \eta_D \tag{25}$$

where $V_{bi}$ is the built-in potential between the channel and source/drain regions.

Equation (23) can be solved as

$$\eta(y) = \frac{\eta_S \sinh[(L_G - y)/\lambda_{gf}] + \eta_D \sinh(y/\lambda_{gf})}{\sinh(L_G/\lambda_{gf})} \tag{26}$$

The location $y_m$ where the potential is minimum can be derived by setting $d\phi_s/dy = 0$. According to Eq. (26), we obtain

$$y_m = \frac{\lambda_{gf}}{2}\left[\frac{\eta_S}{\eta_D}\exp\left(\frac{L_G}{\lambda_{gf}}\right) - 1\right] \Big/ \left[1 - \frac{\eta_S}{\eta_D}\exp\left(-\frac{L_G}{\lambda_{gf}}\right)\right] \tag{27}$$

The $y_m$ is $L_{G/2}$ when $V_D = 0$ and approaches the source region with increasing $V_D$. Substituting Eq. (27) into Eq. (26) and using the approximation $L_G/\lambda_{gf} \gg 1$, we obtain

$$\phi_s(y_m) = V_G' + 2\sqrt{\eta_S\eta_D}\exp\left(-\frac{L_G}{2\lambda_{gf}}\right) - \left\{\frac{\gamma t_{oxf}(V_G' - \phi_{sb})}{\gamma t_{oxf} + \gamma t_{oxb} + t_{si}} + \frac{\gamma t_{oxf}\sigma_p^2(e^{-A^2} - e^{-B^2})(\gamma t_{oxb} + t_{si} + D)}{\lambda_{gf}^2(D + R_p)(\gamma t_{oxf} + \gamma t_{oxb} + t_{si})} \times \frac{qN_p}{\varepsilon_{si}}\right\} \tag{28}$$

The gate voltage where $\phi_s(y_m)$ becomes $2\phi_f$ can be regarded as the threshold voltage and is given by

$$V_{th}' = 2\phi_f + 2\sqrt{\eta_S\eta_D}\exp\left(-\frac{L_G}{2\lambda_{gf}}\right) + \left\{\frac{\gamma t_{oxf}(V_G' - \phi_{sb})}{\gamma t_{oxf} + \gamma t_{oxb} + t_{si}} + \frac{\gamma t_{oxf}\sigma_p^2(e^{-A^2} - e^{-B^2})(\gamma t_{oxb} + t_{si} + D)}{\lambda_{gf}^2(D + R_p)(\gamma t_{oxf} + \gamma t_{oxb} + t_{si})} \times \frac{qN_p}{\varepsilon_{si}}\right\} \tag{29}$$

where $V_{th}' = V_{th} - V_{FB}$.

## 3 Model verification and discussion

The characteristic length shown in Eq. (21) is the key parameter to predict the short-channel effects. It decreases with decreasing device parameters $t_{oxf}$, $t_{si}$, $t_{oxb}$, $R_p$, and $\sigma_p$. This simply means that the short-channel immunity improves accordingly.

The channel doping concentration can be

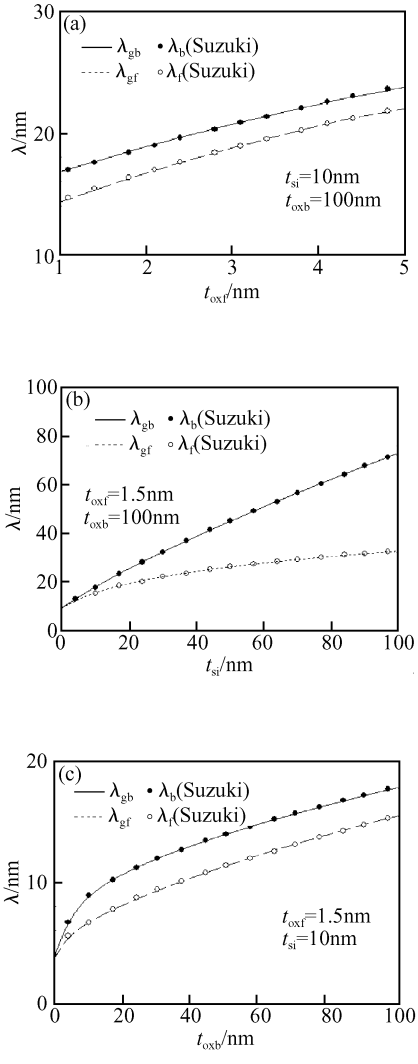


Fig. 2　Dependence of characteristic length on various parameters when $\sigma_p \gg R_p$　(a) $t_{oxf}$; (b) $t_{si}$; (c) $t_{oxb}$

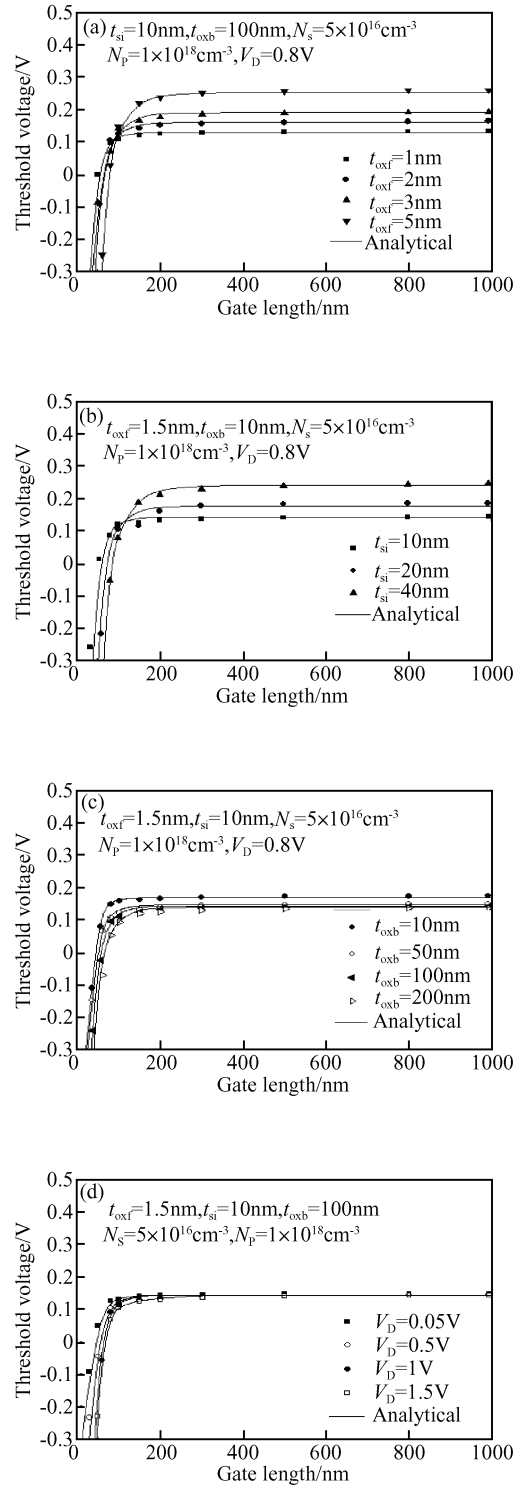


Fig. 3　Dependence of threshold voltage on various parameters　(a) $t_{oxf}$; (b) $t_{si}$; (c) $t_{oxb}$; (d) $V_D$

treated as uniform when $\sigma_p \gg R_p$. Figure 2 shows the dependence of the characteristic length on device parameters $t_{oxf}$, $t_{si}$, and $t_{oxb}$ when $\sigma_p \gg R_p$ and the $\lambda$ is the same as in Suzuki's model. This means our model is also valid for devices with uniform doping profile. The characteristic length associated with back potential is longer than that associated with surface potential. This means the short-channel effects are significant in the bottom of the SOI layer. In Figs. 2(a) and (b), $\lambda_{gf}$ and $\lambda_{gb}$ become close with decreasing $t_{si}$ and $t_{oxb}$.

Figure 3 shows the dependence of the threshold voltage on the gate length with various parameters for retrograde doping. The doping concentration has a Gaussian variation in the film from $N_s = 5 \times 10^{16}\ cm^{-3}$ at the surface to $N_p = 1 \times 10^{18}\ cm^{-3}$ at the back interface. Our model matches well with the numerical data. However it deviates slightly from the numerical data when the roll-off for the threshold voltage is significant. This is due to the assumption that $L_G/\lambda_{gf} \gg 1$ in Eq. (27).

The threshold voltage decreases with decreasing gate oxide thickness, and the short-channel immunity improves accordingly [Fig. 3 (a)]. Therefore a thin gate oxide is more contractive in practice. But if the gate oxide is too thin, a leakage current may occur because of the tunneling effect.

The threshold voltage decreases with decreasing $t_{si}$, and the short-channel immunity improves as a result [Fig. 3(b)]. This is because there is less charge to be coupled by the gate for the devices with a small silicon film thickness. It also shows that the dependence of the threshold voltage on the silicon film thickness is small when the devices have a thin silicon film.

The threshold voltage increases with decreasing buried oxide thickness $t_{oxb}$, and the short-channel immunity improves accordingly [Fig. 3 (c)]. However, the threshold voltage is insensitive to variations in the buried-oxide thickness $t_{oxb}$. The threshold voltage decreases when the drain voltage $V_D$ increases [Fig. 3(d)]. Differentiating Eq. (29) with respect to $V_D$, the drain-induced barrier lowering (DIBL) effect can be evaluated as

$$\mathrm{DIBL} = \frac{\partial V_{th}}{\partial V_D} = \frac{1}{\sqrt{1 + \dfrac{V_D}{\eta_S}}} \exp\left(-\frac{L_G}{2\lambda_{gf}}\right) \quad (30)$$

## 4 Conclusion

Considering 2D effects in both SOI and buried-oxide layers, an analytical model for the threshold voltage by assuming a new potential function perpendicular to the channel for a non-uniform Gaussian doping profile has been proposed. This model has been verified by comparison with MEDICI numerical simulation for the devices with different gate oxide thicknesses, silicon film thicknesses, buried-oxide thicknesses, channel doping concentrations, and drain voltages. Moreover, the characteristic length of our model is equal to Suzuki's when we assume $\sigma_p \gg R_p$. Thus it is also valid for devices with a uniform doping profile.

### References


[1] Zhang Xing, Wang Yangyuan. Design and fabrication of 0.15mm thin film fully depleted MOS/SOI device. Chinese Journal of Semiconductors, 2000, 21(2): 156(in Chinese)[张兴, 王阳元. 0.15μm 薄膜全耗尽 MOS/SOI 器件的设计和研究. 半导体学报, 2000, 21(2): 156]

[2] Liu Xinyu, Sun Haifeng, Liu Hongmin, et al. Fully depleted CMOS/SOI technology. Chinese Journal of Semiconductors, 2003, 24(1): 104(in Chinese)[刘新宇, 孙海峰, 刘洪民, 等. 全耗尽 CMOS/SOI 工艺. 半导体学报, 2003, 24(1): 104]

[3] Young K K. Short-channel effect in fully depleted SOI MOSFETs. IEEE Trans Electron Devices, 1989, 36(2): 399

[4] Yan R H, Ourmzd A, Lee K F. Scaling the Si MOSFET: from bulk to SOI to bulk. IEEE Trans Electron Devices, 1992, 39(7): 1704

[5] Joachim H O, Yamaguchi Y, Ishikawa K, et al. Simulation and two-dimensional analytical modeling of subthreshold slope in ultrathin-film SOI MOSFETs down to 0.1μm gate length. IEEE Trans Electron Devices, 1993, 40(10): 1812

[6] Banna S R, Chan P C H, Ko P K, et al. Threshold voltage model for deep-submicrometer fully depleted SOI MOSFETs. IEEE Trans Electron Devices, 1995, 42(11): 1949

[7] Cheng B J, Shao Z B, Tang T T, et al. Modeling of subthreshold characteristics of deep-submicro-meter FD devices. Chinese Journal of Semiconductors, 2001, 22(7): 908

[8] Suzuki K, Pidin S. Short-channel single-gate SOI MOSFET Model. IEEE Trans Electron Devices, 2003, 50(5): 1297

[9] Sze S M. Physics of semiconductor devices. 2nd ed. New York: wiley, 1983

[10] Ravariu C, Rusu A, Ravariu F, et al. The threshold voltage model of a SOI-MOSFET on films with Gaussian profile. IEEE Conference Proceeding Devices, Circuits and Systems, 2000

[11] Pandey P, Pal B B, Jit S. A new 2-D model for the potential distribution and threshold voltage of fully depleted short-channel Si-SOI MESFETs. IEEE Trans Electron Devices, 2004, 51(2): 24

# 一种非均匀掺杂的全耗尽 SOI-MOSFET 阈值电压模型

张国和†　邵志标　周　凯

（西安交通大学电子科学与技术系，西安　710049）

**摘要**：对垂直于沟道的二维电势分布函数提出了一种新的近似，给出了基于这种近似的杂质浓度呈高斯分布的非均匀掺杂全耗尽 SOI-MOSFET 的阈值电压解析模型.模型结果与 MEDICI 数值模拟结果符合得很好，表明了模型的准确性，这为实践中分析与控制非均匀掺杂的全耗尽 SOI-MOSFET 的阈值电压提供了一种新的途径.

**关键词**：全耗尽 SOI-MOSFET；非均匀掺杂；表面势；阈值电压

**EEACC**：2520M；2560B

**中图分类号**：TN386　　**文献标识码**：A　　**文章编号**：0253-4177(2007)06-0842-06

† 通信作者.Email:ghzhang@stu.xjtu.edu.cn

2006-10-26 收到，2007-01-29 定稿